THE ASTROPHYSICAL JOURNAL, 481:866–871, 1997 June 1

DETECTION OF β PICTORIS–LIKE GASEOUS INFALL IN 2 ANDROMEDAE[1]

K.-P. CHENG[2,3]
Department of Physics, California State University, Fullerton, CA 92634; kcheng@ccvax.fullerton.edu
FRED C. BRUHWEILER
Institute for Astrophysics and Computational Sciences, Department of Physics, Catholic University, Washington, DC 20064
AND
JAMES E. NEFF[2,3]
Department of Astronomy and Astrophysics, Penn State University, University Park, PA 16802
Received 1996 September 24; accepted 1996 December 30

ABSTRACT

Ultraviolet observations of 2 Andromedae with the Goddard High Resolution Spectrograph on board the *Hubble Space Telescope* (*HST*) clearly reveal the existence of circumstellar gas, in addition to previously known anomalous interstellar features, in the line of sight toward this nearby star. We also detect varying, redshifted Ca II absorptions, which we interpret as gaseous infalls. These variable Ca II absorption features and the presence of circumstellar absorptions from Al III $\lambda\lambda$1854.716 and 1862.790 and from excited fine-structure levels of Fe II near 2600 Å seen in 2 And are similar to those observed in spectra of β Pic.

Subject headings: circumstellar matter — ISM: clouds — line: profiles — stars: individual (2 Andromedae) — ultraviolet: stars

1. INTRODUCTION

For the past decade, β Pictoris (spectral type A5 V–IV) has been the subject of intensive imaging and detailed spectroscopic studies. Ultraviolet and visible spectroscopic detections of infalling and outflowing gas surrounding β Pic have raised the possibility that the inner portions of the disk might be undergoing dynamical clearing (Kondo & Bruhweiler 1985; Lagrange, Ferlet, & Vidal-Madjar 1987; Vidal-Madjar et al. 1994). Redshifted circumstellar gas absorption components in β Pic, variable on a short timescale (hours to days), have been interpreted as due to the evaporation of large cometary bodies falling onto the stellar surface (Beust & Tagger 1993; Vidal-Madjar et al. 1994). Nevertheless, the origin and nature of the gaseous disk and the observed infall of β Pic is still not well understood.

During the past 3 years, we have conducted a volume-limited search for β Pic-like systems. Our search included two independent studies: one study looked for circumstellar dust, and the other looked for circumstellar gas around the 62 A stars within 25 pc of the Sun. Using *Infrared Astronomy Satellite* (*IRAS*) data, our survey shows that more than 18% of the nearby A stars have circumstellar dust (Cheng et al. 1992). In our search for circumstellar gas around these A stars, we have identified at least 12 stars with *possible* circumstellar gas based on our high-resolution, high signal-to-noise ratio (S/N) visual spectra and high-dispersion *International Ultraviolet Explorer* (*IUE*) spectra (Neff & Cheng 1995; Cheng & Neff 1997). Among these 12 A stars, only 2 Andromedae has exhibited β Pic-like spectral signatures of gaseous infall, as shown by the new *Hubble Space Telescope* (*HST*) and ground-based spectra we present in this paper.

Both β Pictoris and 2 Andromedae are nearby main-sequence A stars with high $v \sin i$ (Table 1). Since 2 And is a close visual binary (ADS 16467AB) with a period of 76.6 yr and a semimajor axis of 0".277 (Baize & Petit 1989), our ground-based and *HST* observations contain light from both components. However, this double star has a visual magnitude difference of 3.7 mag, and 2 And's companion is possibly a δ Scuti variable with a late A or early F dwarf spectral type. That is, the flux ratio between the primary and the companion in both the Ca II K line and in the ultraviolet wavelength range is greater than 40. Therefore, the fainter companion does not make a significant contribution to our high-resolution spectra of 2 And.

2. OBSERVATIONS

2.1. *Optical High-Resolution* Ca II K *and* Na I D *Spectra of 2 And*

We obtained high resolution ($\lambda/\Delta\lambda \sim 112{,}000$; $\Delta v \sim 2.7$ km s^{-1}) optical spectra of the Ca II K and Na I D lines of 2 And using the National Solar Observatory's 1.5 m McMath-Pierce telescope at Kitt Peak. The echelle grating was used with a TI 800 × 800 CCD detector. A single order was isolated by using a narrow-band interference filter. The aim of these observations was to determine if sharp absorption components were present and to search for mass infall.

The Ca II K (3933.66 Å) spectrum shown in Figure 1 is a co-addition of our 1993 July 26 and July 30 McMath-Pierce observations. The total exposure time was 330 minutes, with S/N ≈ 200 $pixel^{-1}$ at the bottom of the photospheric absorption (which serves as the effective continuum). The Na I D2 (5889.95 Å) spectrum shown in the same figure is a co-addition of four spectra we obtained on the McMath-Pierce on 1993 November 21, with an accumulated exposure time of 120 minutes and with S/N ≈ 400 $pixel^{-1}$ in the adjacent continuum. No variability was seen in the individ-

[1] Based on observations with the NASA/ESA *Hubble Space Telescope* obtained at the Space Telescope Science Institute, which is operated by Association of Universities for Research in Astronomy, Inc., under NASA contract NAS 5-26555.

[2] Guest observer, McDonald Observatory, University of Texas.

[3] Guest observer, National Solar Observatory, NOAO, which is operated by AURA, Inc., under cooperative agreement with the National Science Foundation.

TABLE 1

PROPERTIES OF β PIC AND 2 AND

Star	HD Number	Spectral Type	Distance (pc)	$v \sin i$ (km s^{-1})	Radial Velocity (km s^{-1})
β Pic.......	39060	A5 V–IV	16	139	+20
2 And......	217782	A3 V	19	195	+2

ual data spectra that were co-added to construct the total spectra displayed in Figure 1.

We also used the coudé echelle spectrograph at the McDonald Observatory's 2.7 m telescope ($\lambda/\Delta\lambda \sim 177{,}000$; $\Delta v \sim 1.7$ km s^{-1}) with a TI 800 × 800 CCD detector to monitor 2 And for variable Ca II components. We show two co-added Ca II K spectra obtained at different epochs in Figure 2. The first combined spectrum was obtained on 1994 September 10, with an accumulated exposure time of 180 minutes and S/N ≈ 130 pixel^{-1}. The second combined spectrum was obtained on 1996 August 1 (total exposure time of 200 minutes) and had slightly lower S/N (≈90 pixel^{-1}) because of poor seeing. Again, no evidence was found for spectral variability during each of the observing runs, but we clearly see variable, redshifted circumstellar Ca II when we compare data obtained at the different epochs (Fig. 3).

2.2. *Ultraviolet Spectra of 2 And Obtained with IUE and HST/GHRS*

With our high-resolution Ca II and Na I data, we can detect narrow absorption features due to gas in the line of sight. However, these sharp absorption features, due to transitions from the zero-volt level of abundant ionic species, can arise in either interstellar (IS) or circumstellar (CS) gas. Moreover, the $N_{\mathrm{Na\,I}}/N_{\mathrm{Ca\,II}}$ ratio cannot be used as a direct measure of the physical properties (e.g., temperature and density) of the absorbing gas, even though this ratio is an excellent diagnostic of the depletion of calcium (Vallerga et al. 1993). To discriminate between CS and IS gas and to measure the physical state of the gas, we need to observe diagnostics such as the Fe II lines from fine-structure levels in the resonance UV1 multiplet near 2600 Å (Kondo &

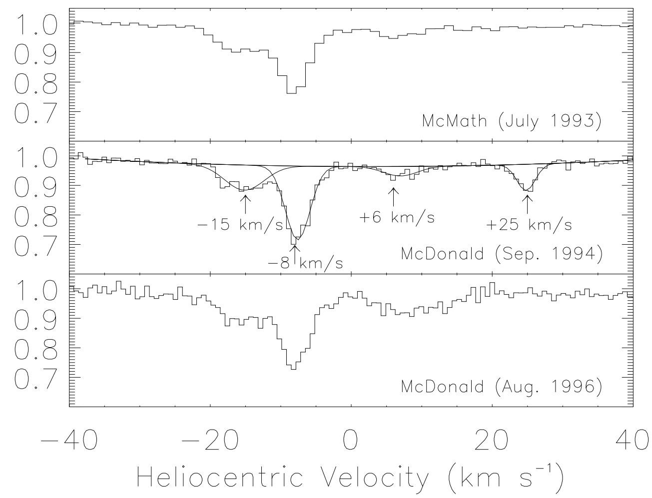

FIG. 2.—Comparison of the high-resolution Ca II K spectra obtained at the McMath-Pierce telescope in 1993 July (*top*) and at the McDonald Observatory 2.7 m telescope in 1994 September (*middle*) and in 1996 August (*bottom*). We interpret the variable feature at +25 km s^{-1} as gaseous infall. This feature was present on spectra obtained two nights apart in 1994 September but was not seen at the other epochs. The broad Ca II feature at +6 km s^{-1} is also variable and could contain both interstellar and circumstellar components.

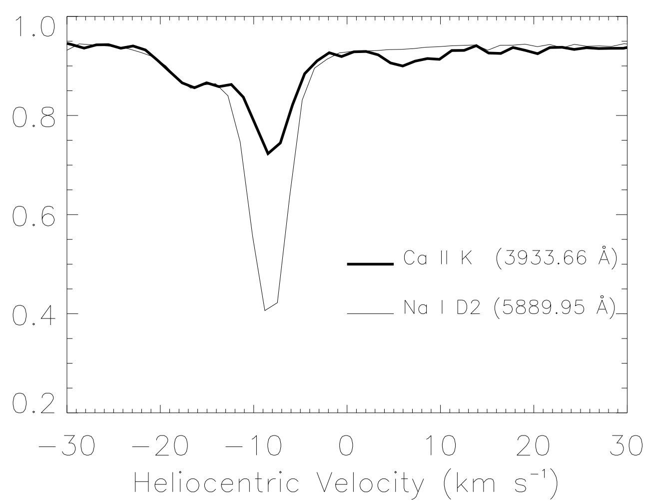

FIG. 1.—Ca II K and Na I D2 spectra ($\lambda/\Delta\lambda \sim 112{,}000$) obtained at the McMath-Pierce telescope. Discrete absorption components are seen in the Ca II K line at −15, −8, and +6 km s^{-1}. Only the −15 and −8 km s^{-1} components are seen in the Na I D lines. There is no significant difference between the Na I profiles obtained on 1993 July 23 and 1993 November 21. The 1993 November data have very weak telluric features in the immediate vicinity of the Na I D lines and no telluric features in the vicinity of the K lines.

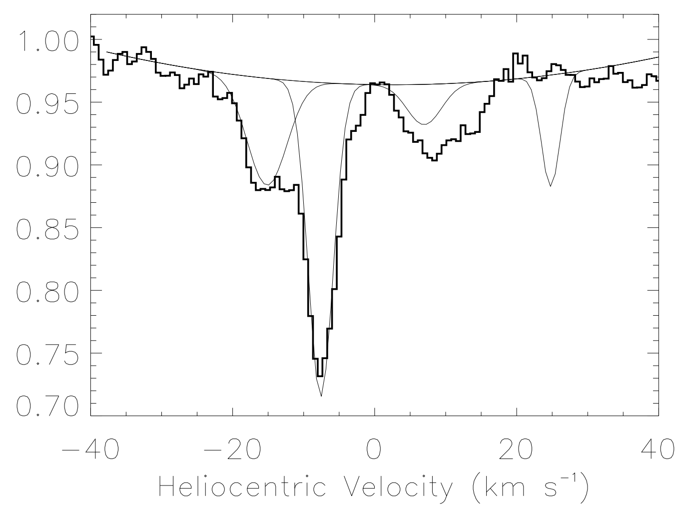

FIG. 3.—High-resolution Ca II K spectra obtained at the McDonald Observatory 2.7 m telescope in 1996 August (*histogram*) compared with the fit to the 1994 September McDonald spectrum. The broad feature at +6 km s^{-1} and the feature at +25 km $^{-1}$ vary substantially between these two epochs.

TABLE 2

LINES OBSERVED TOWARD 2 AND WITH *HST*-GHRS

Species Wavelength[a]	Grating	$\lambda/\Delta\lambda$ (LSA)	Exposure Time (s)
Fe II 2598.370 Å, 2599.396 Å).....................	Echelle B	60,000	435.2
Fe II (2607.087 Å, 2611.870 Å, 2613.825 Å)......	Echelle B	60,000	435.2
Al III (1854.716 Å, 1862.790 Å)	G200M	15,000	598.4

[a] We use air wavelength longward of 2000 Å and vacuum wavelength shortward of 2000 Å.

Bruhweiler 1985) or high-ionization Al III lines (Boggess et al. 1991) at 1854.716 and 1862.790 Å.

Following initial ground-based observations of 2 And that showed multiple absorption components in Ca II, we observed 2 And with the *IUE* at high dispersion (program ID:OD44Z). Multiple exposures, long and short, were obtained in order to have adequate signal-to-noise ratios in both the continuum and in the deep cores of strong photospheric features of the Fe II UV1 resonance multiplet near 2600 Å. Our data revealed only some *possible* circumstellar features in the fine-structure Fe II lines because of the limited S/N of the *IUE* detection.

To verify the presence of circumstellar gas around 2 And and to determine the physical condition in the gas, we observed 2 And again with the Goddard High Resolution Spectrograph (GHRS) on board *HST* on 1995 August 29 (GO program:5876). The spectral regions we observed, using the Large Science Aperture (LSA) with the Echelle B and the G200M gratings, are listed in Table 2. We also obtained one wavelength calibration spectrum for each grating setting in order to achieve accurate registration of our spectra. The radial velocity accuracy is approximately ± 1 km s^{-1} for our Echelle B observations and ± 3 km s^{-1} for the G200M data. The combined increase in resolution and S/N provided by the GHRS data clearly indicate weak circumstellar features in 2 And.

3. DATA REDUCTION AND ANALYSIS

3.1. *Variable, Redshifted Circumstellar* Ca II

Three narrow absorption features were detected in our Ca II K spectrum (see Fig. 2) with heliocentric velocities of $+6$, -8, and -15 km s^{-1}, respectively. However, only the features at -8 and -15 km s^{-1} were seen in our Na I D spectra (Fig. 1). We measured their positions and equivalent widths (Table 3) by fitting Gaussian components to these absorption features and a polynomial to the "background" (i.e., the adjacent photospheric profile).

The Ca II spectrum we obtained at McDonald Observatory on 1994 September 10 revealed a narrow absorption component at $+25$ km s^{-1} that was not seen in our earlier spectra obtained on the McMath-Pierce telescope in 1993 July (Fig. 2). This feature was still present at the same velocity in a spectrum we obtained two nights later. In a spectrum obtained with the same instrumental setup at McDonald on 1996 August 1, the $+25$ km s^{-1} feature was no longer present, but the $+6$ km s^{-1} absorption was more than twice as broad as the absorption seen in the previous epochs and was shifted toward positive velocity (Fig. 3). Both the $+25$ km s^{-1} component and the broad $+6$ km s^{-1} component are redshifted relative to the stellar photospheric velocity, which we interpret as evidence for gaseous infall. This activity is very similar to the variable infall seen in the spectrum of β Pic (Lagrange et al. 1992). On the other hand, β Pic shows a stable feature at the stellar velocity that is not seen in 2 And.

Welty, Morton, & Hobbes (1996) observed the Ca II K lines of 2 And during 1993 September with spectral resolution of 250,000 and S/N $\sim$ 45. With their higher spectral resolution, they were able to resolve our –15 and –8 km s^{-1} features into five individual, narrower components. However, they did not observe the weak but broad feature at $+6$ km s^{-1}, confirming that this feature is variable. Higher resolution observations of the Na I D lines by Welty, Hobbs, & Kulkarni (1994) fail to show the -15 km s^{-1} feature, which is clearly present in both D lines in our data obtained at both epochs. Their data were of much lower S/N (55 vs. 400 for our data), so the feature was probably

TABLE 3

PARAMETERS OF OUR CA II K AND NA I D OBSERVATIONS TOWARD 2 AND

Species	Instrument and Date of Observation	Heliocentric Air Wavelength (Å)	Equivalent Velocity[a] (km s^{-1})	Width (mÅ)	Column Density (cm^{-2})
Ca II K	McMath, 1993 Jul	3933.663	-16	6.7	7.3×10^{10}
	McMath, 1993 Jul		-8	10.8	1.2×10^{11}
	McMath, 1993 Jul		$+6$[b]	1.4	1.5×10^{10}
	McDonald, 1994 Sep		-15	7.0	7.3×10^{10}
	McDonald, 1994 Sep		-8	12.0	1.2×10^{11}
	McDonald, 1994 Sep		$+6$[b]	2.0	1.5×10^{10}
	McDonald, 1994 Sep		$+25$[b]	3.0	3.3×10^{10}
	McDonald, 1996 Aug		-16	9.0	9.8×10^{10}
	McDonald, 1996 Aug		-8	13.0	1.4×10^{11}
	McDonald, 1996 Aug		$+8$[b]	7.0	7.3×10^{10}
Na I D2......	McMath, 1993 Nov	5889.950	-16	9.5	4.9×10^{10}
	McMath, 1993 Nov		-8	38.4	2.0×10^{11}
Na I D1......	McMath, 1993 Nov	5895.924	-15	5.6	5.5×10^{10}
			-8	20.7	2.0×10^{11}

[a] All measurements are in units of ± 1 km s^{-1}.

[b] Observed to be a variable component.

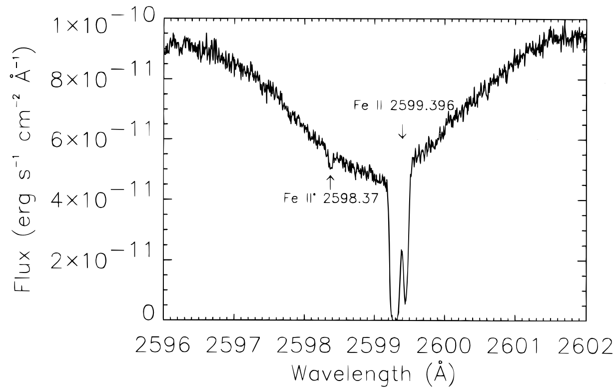

FIG. 4.—GHRS Echelle B spectrum of 2 And obtained on 1995 August 29. The blended absorption lines seen in the core of the Fe II 2599.396 Å photospheric absorption feature could be partly of interstellar and circumstellar origin. The weaker absorption component on the right matches with the Ca II feature at $+6$ km s^{-1}. The stronger component could be a blend of features at -8 and -15 km s^{-1} and is saturated. The Fe II 2598.37 Å feature can only be formed at densities higher than 10^3 cm^3; therefore it must be of circumstellar origin.

lost in the noise. We will continue to monitor both the K and D lines from this system to investigate the potential variability of all of the components.

3.2. *The Circumstellar* Fe II *Lines*

The Fe II lines arising from fine-structure excited J-levels of the resonance UV1 multiplet near 2600 Å are excellent diagnostics of CS gas (Kondo & Bruhweiler 1985; Boggess et al. 1991). Narrow absorption features seen near the core of the Fe II photospheric feature at 2599.396 Å arising from the zero-volt level (Fig. 4) could have both IS and CS contributions. In addition, we clearly detect sharp Fe II absorption features (Fig. 5) from excited J-levels at a wavelength of 2613.825 Å from an excited-state energy of 862.613 cm^{-1} ($J = 3/2$), 2607.088 Å from 667.683 cm^{-1} ($J = 5/2$), and 2598.370 Å and 2611.874 Å from 384.79 cm^{-1} ($J = 7/2$), with measured heliocentric velocities of $\sim 0 \pm 1$ km s^{-1}. This velocity is consistent with the stellar photospheric velocity and suggests that the absorption lines are formed in a stable component of the circumstellar gas surrounding 2 And. As the calculations by Keenan et al. (1988) show, the excited levels in the ground configuration of Fe II are significantly populated and observable only when densities are in excess of 10^3 cm^{-3}. These implied densities are much higher than that of the local interstellar medium near the Sun ($n_H \approx 0.1$ cm^{-3}). Thus, the excited J-level Fe II absorption features displayed in Figure 5 must originate in a high-density region in the immediate circumstellar environment of 2 And.

We used the relative populations of the ground state and excited fine-structure levels of Fe II (Keenan et al. 1988) to constrain both temperature and electron density in the circumstellar gas around 2 And. We first determined the column densities of Fe II lines arising from the $^6D_{7/2}$ state (2611.874 Å), the $^6D_{5/2}$ state (2607.088 Å), and the $^6D_{3/2}$ state (Fe II 2613.825 Å) from their equivalent widths (see Table 4) by assuming that all the equivalent widths lay on the linear portion of the curve of growth. We then compared the derived column densities of $N(\mathrm{Fe}^J$ II$) = 1.27 \times 10^{12}$ cm^{-2} ($J = 7/2$), 7.76×10^{11} cm^{-2} ($J = 5/2$), and 6.45×10^{11} cm^{-2} ($J = 3/2$) with the predicted relative populations as a function of n_e and T for these levels (Keenan et al. 1988). Although these derived numbers are sensitive to the accuracy of our equivalent width measurements and f-values, our calculated relative populations of the $^6D_{7/2}$, $^6D_{5/2}$, and $^6D_{3/2}$ levels (1.00:0.61:0.51) demonstrate that the density must be $\geq 10^6$ cm^{-3} for any reasonable estimate of the temperature. At densities above 10^6 cm^{-3}, the relative populations are determined by a Boltzmann distribution, so the predicted relative populations for the $J = 7/2$, 5/2, and 3/2 levels yield a lower limit to the characteristic density of the CS gas producing the Fe II absorption. Besides this lower density limit, we also find that the temperature of the CS gas around 2 And must be between 3000 K and 10,000 K to give rise to the observed Fe II relative populations.

Using the circumstellar gas temperature range derived for Fe II, we obtain a total circumstellar Fe II column density of

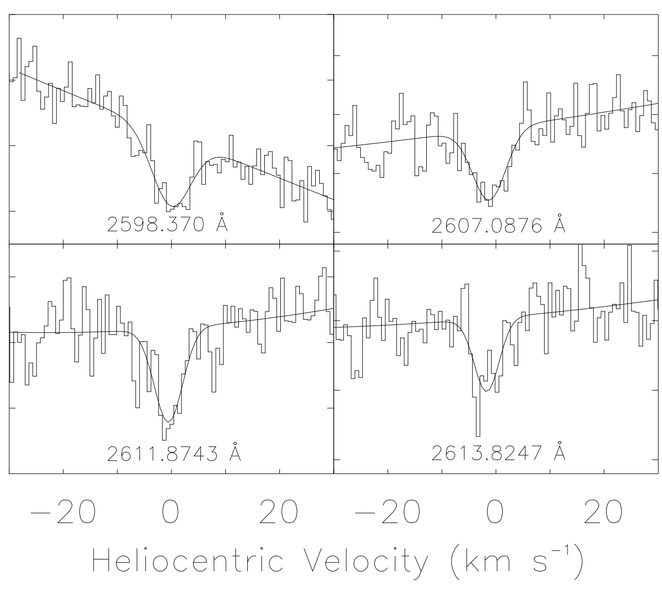

FIG. 5.—Fe II lines from excited J-levels of the resonance UV1 multiplet near 2600 Å are excellent diagnostics of circumstellar gas. We clearly detect sharp absorption features from excited J-levels of Fe II at 2598.370, 2607.0876, 2611.8743, and 2613.8247 Å. The heliocentric velocity of each of these features is $\sim 0 \pm 1$ km s^{-1}, which suggests that the features arise in a stable circumstellar component.

TABLE 4

PARAMETERS OF OUR OBSERVATIONS TOWARD 2 AND WITH *HST*

Lines[a]	Wavelength[b] (Å)	Heliocentric Velocity (km s^{-1})	Equivalent Width (mÅ)	Column Density (cm^{-2})
CS, Fe II (384.79 cm^{-1})	2598.370	-0.1 ± 1	7 ± 1	1.2×10^{12}
IS + CS, Fe II (0 cm^{-1})	2599.396	-5 to -15	150[c]	...
IS + CS, Fe II (0 cm^{-1})	2599.396	$+5.7 \pm 1$	79 ± 1	1.2×10^{13}
CS, Fe II (667.683 cm^{-1})	2607.088	-1.0 ± 1	5.3 ± 1	7.76×10^{11}
CS, Fe II (384.790 cm^{-1})	2611.874	-0.6 ± 1	8.6 ± 1	1.27×10^{12}
CS, Fe II (862.613 cm^{-1})	2613.825	-0.3 ± 1	4.0 ± 1	6.45×10^{11}
CS, Al III (53916.6 cm^{-1})......	1854.716	0 ± 3	15 ± 5	8.73×10^{11}

[a] Entries give where the line is found, its ionic species, and its excited-state energy.
[b] We use air wavelength longward of 2000 Å and vacuum wavelength shortward of 2000 Å.
[c] Total equivalent width of at least two blended components.

4.79×10^{12} $cm^{-2} \leq N$(Fe II) $\leq 4.93 \times 10^{12}$ cm^{-2}. Adopting lower gas temperatures will increase the total Fe II column density. If we further adopt the solar abundance ratio $n(\text{Fe})/n(\text{H}) = 3.23 \times 10^{-5}$ (Anders & Grevesse 1989) and N(Fe II) $\approx N$(Fe), our results imply a corresponding range for the total hydrogen column density of 1.48×10^{17} $cm^{-2} \leq N(\text{H}) \leq 1.53 \times 10^{17}$ cm^{-2} along the line of sight through the CS gas. If part of the Fe is depleted onto grains, the H I column density could be significantly higher. In any event, this value is much less than the CS gas column density for β Pic of 1×10^{18} $cm^{-2} \leq N(\text{H}) \leq 4 \times 10^{20}$ cm^{-2} deduced by Hobbs et al. (1985) using Zn and Ca lines.

The amount of circumstellar gas around 2 And could be more than we estimate above. Since the velocity (+6 km s^{-1}) of the weaker absorption line seen in the core of Fe II 2599.396 Å ($J = 9/2$) photospheric absorption (Fig. 4) matches that of the variable Ca II K line seen at +6 km s^{-1} (Fig. 3), this Fe II absorption from the ground-state ($J = 9/2$ level) could be, at least in part, of circumstellar origin. We therefore attempted to estimate the column density of the +6 km s^{-1} Fe II 2599.396 Å component and the upper limit of the gas density giving rise to this absorption at +6 km s^{-1}. By fitting multiple Voigt profiles to the Fe II 2599.396 Å line, we reconstructed the total Fe II absorption complex seen in Figure 4. In fitting the GHRS spectrum, we used the individual IS cloud velocities (−15 km s^{-1}, −8 km s^{-1}, and +6 km s^{-1}) determined from our high-resolution Ca II spectra. The CS velocity (−1 km s^{-1}) and Fe II ($J = 9/2$) column density (1.5×10^{12} cm^{-2}) used in the fitting were derived from the Fe II 2598.370 Å and 2611.874 Å lines and the predicted relative populations of the Fe II J-levels (Keenan et al. 1998). The resulting column density of the zero-volt $^6D_{9/2}$ level of Fe II line at +6 km s^{-1} was $\sim 1.2 \times 10^{13}$ cm^{-2}. We emphasize that this column density is a qualitative estimate because the component at +6 km s^{-1} approaches saturation and is very sensitive to the fitting parameters. If our estimate for the Fe II zero-volt component at +6 km s^{-1} is reasonable, the nondetection of corresponding excited J-level Fe II lines at the same velocity implies that the absorbing gas has density $\leq 10^{3.5}$ cm^{-3} (see Keenan et al. 1988 for the relative populations). This upper limit does not impose strong constraints and does not rule out the possibility that the absorption at +6 km s^{-1} has an interstellar component.

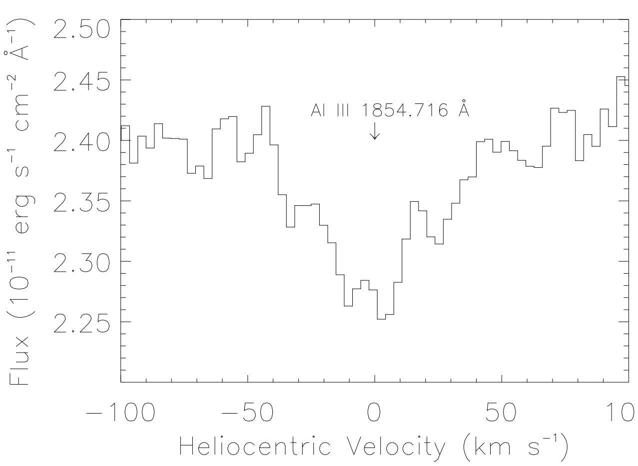

FIG. 6.—The circumstellar Al III line at 1854.716 Å seen in our G200M spectrum with heliocentric velocity near 0 km s^{-1}. Because of the poor S/N in our short G200M exposure, the weaker line at 1862.790 Å (not shown here) of this resonance doublet was only marginally detected.

3.3. *The Circumstellar* Al III *Lines*

We detect weak absorption features in our GHRS/G200M spectrum that correspond to Al III 1854.716 and 1862.790 Å with heliocentric velocities of 0 ± 3 km s^{-1} (Fig. 6). Since the weaker Al III 1862.790 Å is only marginally detected due to the poor S/N in our short G200M exposure, our determination of the Al III column density is based solely on the strength of the stronger Al III line. Assuming the measured equivalent width of the Al III 1854.716 Å, 15 ± 5 mÅ, lies on the linear portion of the curve of growth, we derive $N(\text{Al III}) = 8.7 \pm 2.9 \times 10^{11}$ cm^{-2}.

The ionization potential required to produce Al III is 18.828 eV. This ionization is too high for Al III to be produced in the photospheres of A stars, such as β Pic and 2 And, that have effective temperatures $T_{\text{eff}} \leq 10{,}000$ K. Furthermore, these stars do not have nearly enough photoionizing flux to yield the necessary ionization in their circumstellar envelopes. These highly ionized species could be either produced in a shocked region above the stellar surface (Bruhweiler, Kondo, & Grady 1991) or produced by falling evaporating comets (Beust & Tagger 1993).

4. DISCUSSION

Based on our observations of 2 Andromedae and β Pictoris, which show infalling circumstellar gas and highly ionized gas (e.g., Al III) for both stars, we conclude that β Pic is not unique.

Both 2 And (Andrillat, Jaschek, & Jaschek 1995) and β Pic (King & Patten 1992) have been classified as λ Boo stars, which are a small group of A-type stars with spectral peculiarities, such as large metal deficiency (weak metallic lines), rapid rotation (~ 100 km $^{-1}$), and Population I kinematics. Venn & Lambert (1990) suggested that λ Boo stars are created when circumstellar gas is separated from the grains (the bulk of the grains comprise a circumstellar disk that is detectable by its IR radiation) and is accreted onto the star. However, we think there is no link between the circumstellar dust and the gaseous spectroscopic events we observed in either β Pic or 2 And. Based on our *IRAS* study of nearby A stars (Cheng et al. 1992), 2 And exhibits no *IRAS* detectable IR excess at either 25 or 60 μm, while β Pic has a large IR excess in both bandpasses. A relatively dust-free λ Boo star with accreting gas poses problems for models used to explain the metal deficiency in λ Boo stars.

Finally, our detection of a circumstellar gas envelope about 2 And may have implications for the anomalously strong, presumably interstellar Mg I line (Frisch et al. 1990) and for the high $N_{\rm Na\ I}/N_{\rm Ca\ II}$ ratio of 2.47 (Welsh et al. 1991) seen toward this star. Our detection of circumstellar gas in 2 And certainly suggests that one must be careful in the interpretation of what might first appear to be interstellar features. Moreover, our nonrestrictive upper limit for the $+6$ km s^{-1} feature of Fe II 2599.396 indicates that it is quite difficult to distinguish between interstellar and circumstellar features even with high-quality data.

We thank our referee for constructive comments. We also would like to thank staff members of the Solar-Stellar Program at the National Solar Observatory and the staff of the McDonald Observatory for their assistance. Support for this work was provided by NASA through grant number GO-5876 from the Space Telescope Science Institute, which is operated by AURA, Inc., under NASA contract NAS 5-26555, and by NSF grant AST 95-20989 to the California State University at Fullerton. This research made use of the SIMBAD database, operated at CDS, Strasbourg, France.

REFERENCES

Anders, E., & Grevesse, N. 1989, Geochim. Cosmochim. Acta, 53, 197

Andrillat, Y., Jaschek, C., & Jaschek, M. 1995, A&A, 299, 493

Baize, P., & Petit, M. 1989, A&AS, 77, 497

Beust, H., & Tagger, M. 1993, Icarus, 106, 42

Boggess, A., Bruhweiler, F. C., Grady, C. A., Ebbets, D. C., Kondo, Y., Trafton, L. M., Brandt, J. C., & Heap, S. R. 1991, ApJ, 377, L49

Bruhweiler, F. C., Kondo, Y., & Grady, C. A. 1991, ApJ, 371, L27

Cheng, K.-P., Bruhweiler, F. C., Kondo, Y., & Grady, C. A. 1992, ApJ, 396, L83

Cheng, K.-P., & Neff, J. E. 1997, in preparation

Frisch, P. C., Welty, D. E., York, D. G., & Fowler, J. R. 1990, ApJ, 357, 514

Hobbs, L. M., Vidal-Madjar, A., Ferlet, R., Albert, C. E., & Gry, C. 1985, ApJ, 293, L29

Keenan, F. P., Hibbert, A., Burke, P. G., & Berrington, K. A. 1988, ApJ, 332, 539

King, J. R., & Patten, B. M. 1992, MNRAS, 256, 571

Kondo, Y., & Bruhweiler, F. C. 1985, ApJ, 291, L1

Lagrange, A. M., Ferlet, R., & Vidal-Madjar, A. 1987, A&A, 173, 289

Lagrange, A. M., Gosset, E., Beust, H., Ferlet, R., & Vidal-Madjar, A. 1992, A&A, 264, 637

Neff, J. E., & Cheng, K.-P. 1995, Ap&SS, 224, 525

Vallerga, J. V., Vedder, P. W., Craig, N., & Welsh, B. Y. 1993, ApJ, 411, 729

Venn, K. A., & Lambert, D. L. 1990, ApJ, 363, 234

Vidal-Madjar, A., et al. 1994, A&A, 290, 245

Welty, D. E., Hobbs, L. M., & Kulkarni, V. P. 1994, ApJ, 436, 152

Welsh, B. Y., Vedder, P. W., Vallerga, J. V., & Craig, N. 1991, ApJ, 381, 462

Welty, D. E., Morton, D. C., & Hobbs, L. M. 1996, ApJS, 106, 533